

# VARIABLE GAMMA-RAY EMISSION FROM THE CRAB NEBULA: SHORT FLARES AND LONG “WAVES”

E. STRIANI<sup>1,2,3</sup>, M. TAVANI<sup>1,2,3</sup>, V. VITTORINI<sup>1</sup>, I. DONNARUMMA<sup>1</sup>, A. GIULIANI<sup>5</sup>, G. PUCCELLA<sup>4</sup>, A. ARGAN<sup>1</sup>,  
A. BULGARELLI<sup>6</sup>, S. COLAFRANCESCO<sup>11,12</sup>, M. CARDILLO<sup>1,2</sup>, E. COSTA<sup>1</sup>, E. DEL MONTE<sup>1</sup>, A. FERRARI<sup>8</sup>, S. MEREGHETTI<sup>5</sup>,  
L. PACCIANI<sup>1</sup>, A. PELLIZZONI<sup>9</sup>, G. PIANO<sup>1</sup>, C. PITTORI<sup>10</sup>, M. RAPISARDA<sup>4</sup>, S. SABATINI<sup>1</sup>, P. SOFFITTA<sup>1</sup>, M. TRIFOGLIO<sup>6</sup>,  
A. TROIS<sup>9</sup>, S. VERCELLONE<sup>7</sup>, F. VERRECCHIA<sup>10</sup>

*Published by Astrophysical Journal, Volume 765, 52 (Feb. 2013)*

## ABSTRACT

Gamma-ray emission from the Crab Nebula has been recently shown to be unsteady. In this paper, we study the flux and spectral variability of the Crab above 100 MeV on different timescales ranging from days to weeks. In addition to the four main intense and day-long flares detected by AGILE and Fermi-LAT between Sept. 2007 and Sept. 2012, we find evidence for week-long and less intense episodes of enhanced gamma-ray emission that we call “waves”. Statistically significant “waves” show timescales of 1-2 weeks, and can occur by themselves or in association with shorter flares. We present a refined flux and spectral analysis of the Sept. - Oct. 2007 gamma-ray enhancement episode detected by AGILE that shows both “wave” and flaring behavior. We extend our analysis to the publicly available Fermi-LAT dataset and show that several additional “wave” episodes can be identified. We discuss the spectral properties of the September 2007 “wave”/flare event and show that the physical properties of the “waves” are intermediate between steady and flaring states. Plasma instabilities inducing “waves” appear to involve spatial distances  $l \sim 10^{16}$  cm and enhanced magnetic fields  $B \sim (0.5 - 1)$  mG. Day-long flares are characterized by smaller distances and larger local magnetic fields. Typically, the deduced total energy associated with the “wave” phenomenon ( $E_w \sim 10^{42}$  erg, where  $E_w$  is the kinetic energy of the emitting particles) is comparable with that associated to the flares, and can reach a few percent of the total available pulsar spindown energy. Most likely, flares and waves are the product of the same class of plasma instabilities that we show acting on different timescales and radiation intensities.

*Subject headings:*

## 1. INTRODUCTION

The Crab Nebula (the remnant of a Supernova explosion witnessed by Chinese astronomers in 1054) is powered by a very powerful pulsar (of period  $P = 0.33$  ms, and spindown luminosity  $L_{sd} \simeq 5 \times 10^{38}$  erg s<sup>-1</sup>) (see e.g., Hester 2008). The pulsar is energizing the whole system through the interaction of the particle and wave output within the surrounding Nebula (of average magnetic field  $\sim 200 \mu$ G). The resulting unpulsed emission from radio to gamma rays up to 100 MeV is interpreted as synchrotron radiation from at least two populations of electrons/positrons energized by the pulsar wind and by surrounding shocks or plasma instabilities (e.g., Atoyan & Aharonian 1996, Meyer et al. 2010). The optical and X-ray brightness enhancements observed in the inner Nebula, known as “wisps”, “knots”, and the “anvil” aligned with the pulsar “jet” (Scargle 1969; Hester 1995, 2008; Weisskopf 2000), show flux variations on timescales of weeks or months. On the other hand, the average unpulsed emission from the Crab Nebula was always con-

sidered essentially stable. The surprising discovery by the AGILE satellite of variable gamma-ray emission from the Crab Nebula in Sept. 2010 (Tavani et al. 2010; Tavani et al. 2011a), and the Fermi-LAT confirmation (Buehler et al. 2010; Abdo et al. 2011) started a new era of investigation of the Crab system. As of Sept. 2012 we know of four major gamma-ray flares from the Crab Nebula detected by the AGILE Gamma-Ray Imaging Detector (GRID) and Fermi-LAT: (1) the Sept-Oct. 2007 event, (2) the Feb. 2009 event, (3) the Sept. 2010, and (4) the “super-flare” event of Apr. 2011 (Buehler et al. 2011; Tavani et al. 2011b; Hays et al. 2011; Striani et al. 2011a; Striani et al. 2011b; Buehler et al. 2012).

In this paper we address the issue of the gamma-ray variability of the Crab Nebula on different timescales ranging from days to weeks. We then enlarge the parameter space sampled by previous investigations especially for the search of statistically significant enhanced emission on timescales of 1-2 weeks. Sect. 2 presents a brief overview of the current knowledge on Crab’s main gamma-ray flares. Sect. 3 presents the results of a search of  $\gamma$ -ray enhanced emission on timescales of weeks in the AGILE database. We also discuss in detail the Sept.-Oct. 2007 event detected by AGILE which shows a strong evidence of short timescale flaring as well as substantial emission on longer timescales of order of 1 week. Sect. 4 presents the results of our search for long and short timescale enhanced emission in the available Fermi-LAT data. In both the  $\gamma$ -ray telescopes data we find strong evidence of week-long  $\gamma$ -ray enhanced emission episodes at intermediate peak intensities that we call “waves”. Sect. 5 presents the physical implications of our findings in terms of a synchrotron emission model. We discuss in Sect. 6 the main implications of our work.

<sup>1</sup> INAF/IASF-Roma, I-00133 Roma, Italy

<sup>2</sup> Dip. di Fisica, Univ. Tor Vergata, I-00133 Roma, Italy

<sup>3</sup> INFN Roma Tor Vergata, I-00133 Roma, Italy

<sup>4</sup> ENEA Frascati, I-00044 Frascati (Roma), Italy

<sup>5</sup> INAF/IASF-Milano, I-20133 Milano, Italy

<sup>6</sup> INAF/IASF-Bologna, I-40129 Bologna, Italy

<sup>7</sup> INAF-IASF Palermo, Palermo, Italy

<sup>8</sup> CIFS-Torino, I-10133 Torino, Italy

<sup>9</sup> INAF-Osservatorio Astronomico di Cagliari, localita’ Poggio dei Pini, strada 54, I-09012 Capoterra, Italy

<sup>10</sup> ASI Science Data Center, I-00044 Frascati(Roma), Italy

<sup>11</sup> INAF - Osservatorio Astronomico di Roma via Frascati 33, I-00040 Monteporzio, Italy.

<sup>12</sup> University of the Witwatersrand, Private Bag 3, 2054 South Africa

TABLE 1  
TABLE OF THE flares ( $F \geq 700 \times 10^{-8} \text{ ph cm}^{-2} \text{ s}^{-1}$ ) OF THE CRAB NEBULA FOUND IN THE AGILE AND FERMI DATA FROM SEPT. 2007.

	Name	MJD	$\tau_1$ (hr)	$\tau_2$ (hr)	Peak Flux	$B(mG)$	$\gamma^*$ ( $10^9$ )	$l$ ( $10^{15}$ cm)
2007 (AGILE)	$F_1$	54381.5	$22 \pm 11$	$10 \pm 5$	$1000 \pm 150$	$1.0 - 2.0$	$2.6 - 4.8$	$1.2 - 3.6$
	$F_2$	54382.5	$14 \pm 7$	$6 \pm 3$	$1400 \pm 200$	$1.1 - 2.1$	$2.3 - 4.3$	$0.8 - 2.2$
	$F_3$	54383.7	$11 \pm 5$	$14 \pm 7$	$900 \pm 150$	$1.0 - 2.0$	$2.6 - 4.8$	$0.8 - 1.7$
2009 (FERMI)	$F_4$	54865.8	$10 \pm 5$	$20 \pm 10$	$700 \pm 140$	$0.7 - 1.3$	$2.6 - 4.8$	$0.6 - 1.6$
	$F_5$	54869.2	$10 \pm 5$	$22 \pm 11$	$830 \pm 90$	$0.8 - 1.4$	$2.6 - 4.8$	$0.6 - 1.6$
2010 (AGILE & FERMI)	$F_6$	55457.8	$8 \pm 4$	$22 \pm 11$	$850 \pm 130$	$0.7 - 1.3$	$2.5 - 4.7$	$0.5 - 1.3$
	$F_7$	55459.8	$6 \pm 3$	$6 \pm 3$	$1000 \pm 100$	$1.4 - 2.6$	$2.6 - 4.8$	$0.3 - 0.9$
	$F_8$	55461.9	$19 \pm 10$	$8 \pm 4$	$750 \pm 110$	$0.8 - 1.4$	$2.5 - 4.8$	$0.9 - 3.1$
2011 (FERMI & AGILE)	$F_9$	55665.0	$9 \pm 5$	$9 \pm 5$	$1480 \pm 80$	$1.2 - 2.2$	$2.8 - 5.0$	$0.5 - 1.5$
	$F_{10}$	55667.3	$10 \pm 5$	$24 \pm 12$	$2200 \pm 85$	$1.3 - 2.3$	$2.7 - 4.9$	$0.6 - 1.6$

The timescales  $\tau_1$  and  $\tau_2$  are the rise and decay timescales of the flares modelled with an exponential fit respectively. The characteristic length of the emitting region is deduced from the relation  $l = c\delta\tau_1$ . The Lorentz factor  $\gamma^*$  characterizes the adopted model of the accelerated particle distribution function  $dn/d\gamma = K/\alpha \cdot \delta(\gamma - \gamma^*)$ , where  $K$  is defined in the spherical approximation.  $\alpha = 1$  in the spherical case, and  $\alpha < 1$  for cylindrical or pancake-like volumes reproducing the current sheet geometry. The peak photon flux above 100 MeV is measured in units of  $10^{-8} \text{ ph cm}^{-2} \text{ s}^{-1}$ . These parameters are obtained, by means of a multi-parameter fit, from the following quantities (in the observer frame): the position of the peak photon energy,  $E_p \propto \delta\gamma^{*2}B$ , the peak emitted power  $\nu F \propto \delta^4 K/\alpha l^3 B^2 \gamma^{*2}$ , the rise time  $\tau_1 = l/(c\delta)$ , and the cooling time  $\tau_2 = 8.9 \times 10^3 / [(B/\text{Gauss})^2 \gamma^{*2} \delta]$ , assuming  $\delta = 1$  (see text).

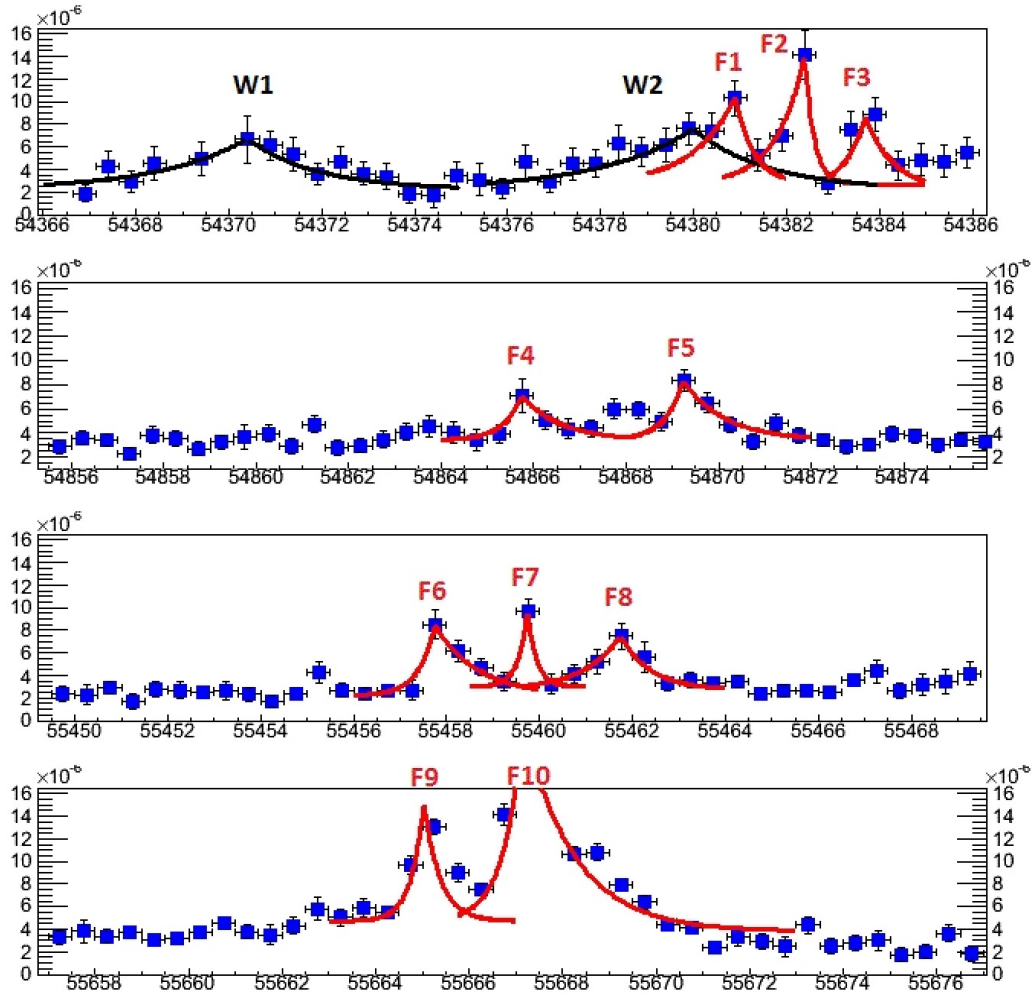


FIG. 1.— Gamma-ray lightcurves above 100 MeV (12-hr time bins) from the Crab (pulsar plus Nebula) detected by AGILE and Fermi-LAT. From top to bottom, the Sept. - Oct. 2007 event (AGILE data), the Feb. 2009 event (Fermi-LAT data), the Sept. 2010 event (Fermi-LAT data), and the Apr. 2011 event (Fermi-LAT data).

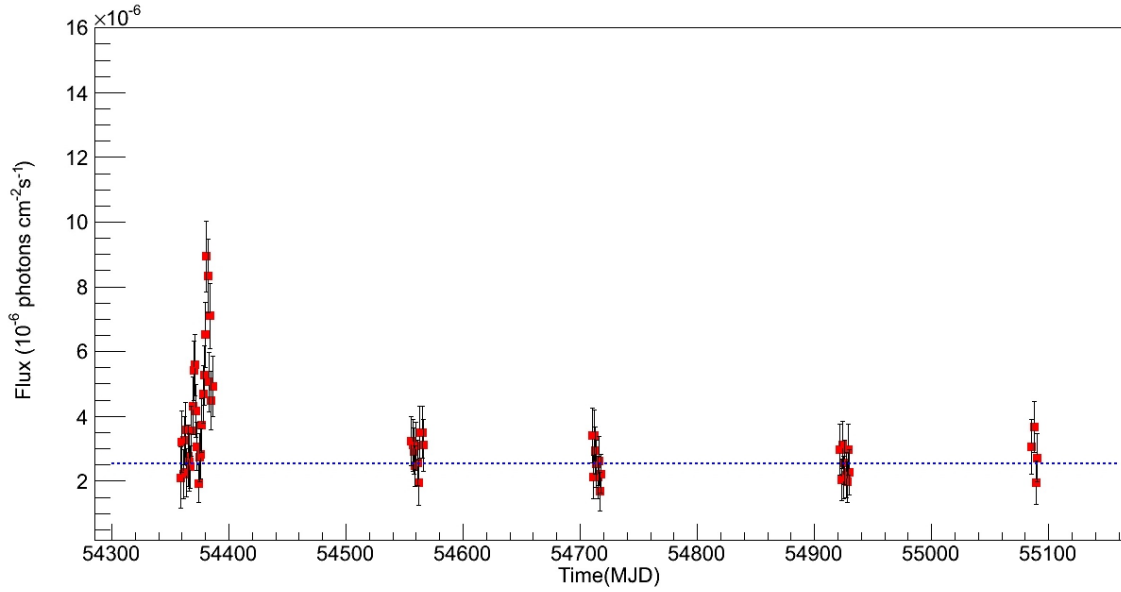


FIG. 2.— Gamma-ray 1-day binned lightcurve above 100 MeV of the five AGILE observations of the Crab Nebula in pointing mode, from Sept. 2007 to Oct. 2009. The gamma-ray flux enhancement during the September-October 2007 pointing (MJD = 54366 - 54386) is evident.

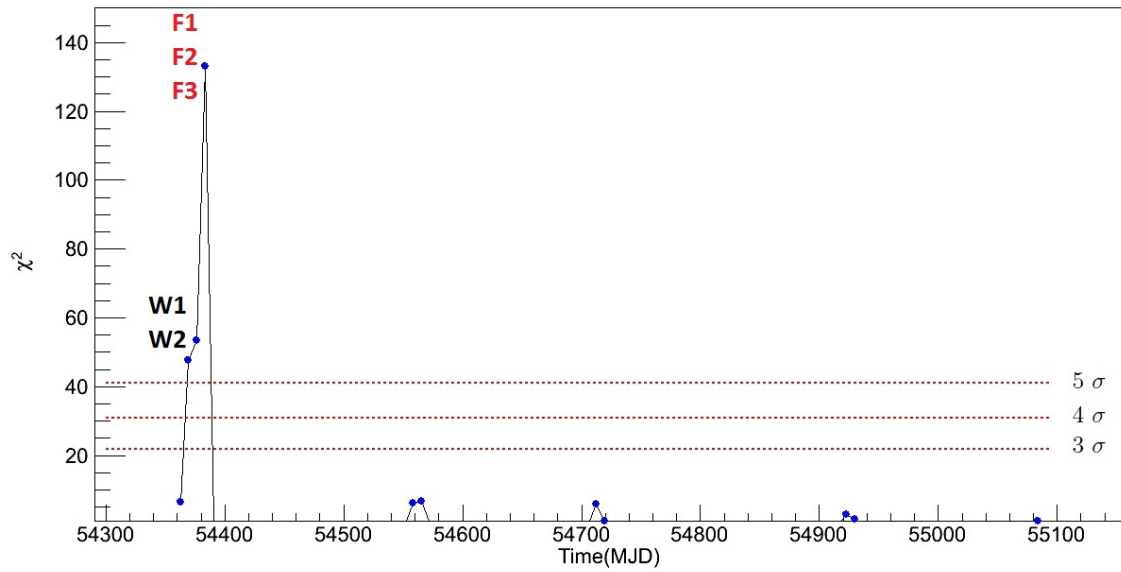


FIG. 3.— Plot of the  $\chi^2$  values (each calculated for 7-day time intervals based on 1-day binned data) as a function of time for the AGILE data on the Crab covering the period Sept. 2007/Oct. 2009 in pointing mode. The red dashed lines indicate the  $\chi^2$  corresponding to the  $3\sigma$ ,  $4\sigma$  and  $5\sigma$  confidence level.

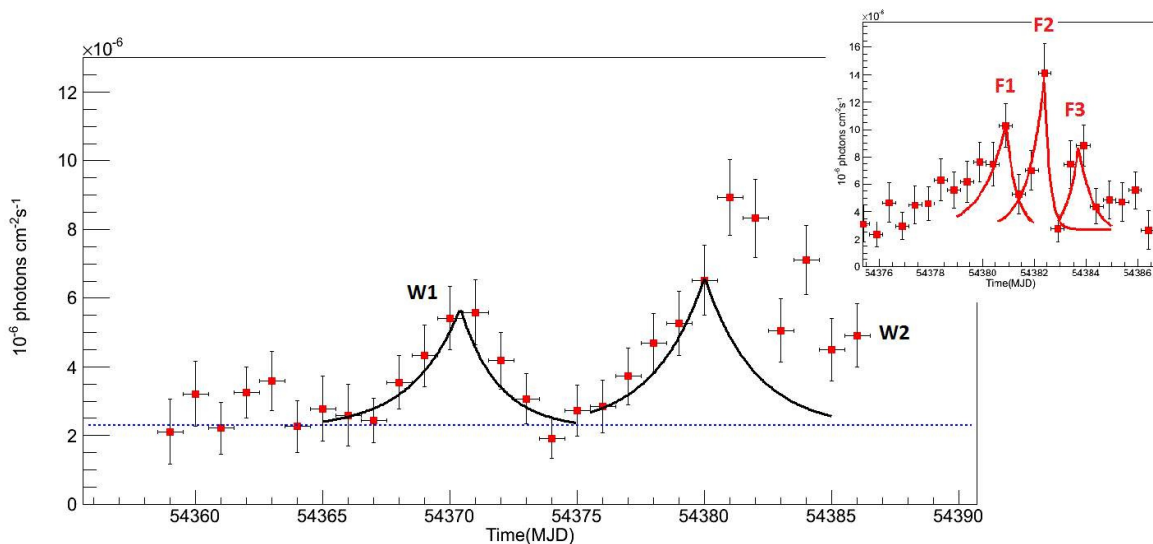


FIG. 4.— Lightcurve (1-day bin) of the Sept.- Oct. 2007 Crab Nebula flare detected by AGILE. In the inset the 12-hr bin lightcurve around the flare. This episode is characterized by a very strong variability, with waves (black line, marked with a *W*) and flares (red line, marked with an *F*).

## 2. OVERVIEW OF THE MAIN GAMMA-RAY FLARES

Four major episodes of intense gamma-ray flaring from the Crab Nebula have been detected by AGILE and Fermi-LAT (Tavani et al. 2011a; Abdo et al. 2011; Striani et al. 2011b; Vittorini et al. 2011; Buehler et al. 2012). The definition of a “flare” adopted in this paper is that of a single gamma-ray enhancement event with a risetime  $\tau_1 < 1$  day and flux  $F > 700 \times 10^{-8} \text{ ph cm}^{-2} \text{ s}^{-1}$  above 100 MeV. Table 1 summarizes the flaring events that we find by considering the AGILE and the publicly available Fermi-LAT database. These events show a complex time structure, being composed of several sub-flares that we classify as  $F_n$ , with  $n$  a progressive number. Fig. 1 summarizes the four major flaring episodes with the same temporal and flux scales. The colored curves are indicative of the flaring behavior that in most cases can be represented by an exponential fit<sup>13</sup>(e.g., Norris et al. 1996), characterized by rising ( $\tau_1$ ) and decay ( $\tau_2$ ) timescales as given in Table 1. We also report in Table 1 the data fitting physical parameters (average local magnetic field  $B$ , typical particle Lorentz factor  $\gamma^*$ , and characteristic size  $l$  of the emitting region of the flaring episodes). We determine these parameters and their uncertainties from the time constants  $\tau_1$  and  $\tau_2$  (see discussion below). Whenever applicable (2010 and 2011 events), the AGILE and Fermi-LAT data are consistent both in flux and spectral properties.

Motivated by the claim of fast variability in the September 2010 event (Balbo et al. 2011) and the dramatic detection of the short timescale variability in the Crab gamma-ray flare of April 2011 (Buehler et al. 2011),

<sup>13</sup> We use the fitting function

$$f = \begin{cases} F_b + A \exp(-|t - t_p|/\sigma_1) & \text{for } t \leq t_p \\ F_b + A \exp(-|t - t_p|/\sigma_2) & \text{for } t > t_p \end{cases}$$

where  $F_b$  is the flux baseline,  $A$  a flux parameter,  $t_p$  is the peak time,  $\sigma_1$  and  $\sigma_2$  the rise and decay time constants. The rise and decay times, half to maximum amplitude, are obtained as  $\tau_{1,2} = [\ln(2)] \sigma_{1,2}$ .

we revisited the analysis of the Crab flare detected by Fermi in Feb. 2009, and the AGILE and Fermi analysis of the September 2010 event (12-hr bin lightcurve for  $E > 100$  MeV, first two panels of Fig. 1). This revised analysis shows for both the 2009 and 2010 events a sequence of three flares, that could not be previously appreciated with a 2-day time bin. Regarding the September 2010 event, both the AGILE data and the Fermi-LAT data agree quite well, and are consistent with the analysis presented in Balbo et al. 2011.

## 3. THE SEPTEMBER-OCTOBER 2007 EVENT DETECTED BY AGILE

The Crab pulsar plus Nebula is a primary source for gamma-ray calibration, and AGILE pointed at the source several times during the pointing mode phase from July 2007 until Oct. 2009 for different geometries and off-axis angles. The ideal periods during the year for AGILE pointings of the Crab region are September-October and March-April as determined by the solar panel constraints. Fig. 2 shows the overall gamma-ray lightcurve collecting all the available AGILE observations which includes several pointings in 2007, 2008 and 2009. Typically, pointing observations lasted  $\sim 10$  days, except for the initial pointing in September-October 2007 that was substantially longer.

During this first pointing, indeed, we detected an episode of enhanced gamma-ray emission. A preliminary lightcurve of this episode, performed with a 1-day bin, was presented in Tavani et al. 2011a. In that study we reported a quite long episode (about 2 weeks) of enhanced emission with a 1-day peak flux of  $F_p = (890 \pm 110) \times 10^{-8} \text{ ph cm}^{-2} \text{ s}^{-1}$  above 100 MeV.

Fig. 2 shows the 1-day lightcurve ( $E > 100$  MeV) of the Crab (pulsar plus Nebula) extended to the five observations of the Crab Nebula performed by AGILE during the pointing mode. In order to search for statistically significant enhanced gamma-ray emission on timescales of weeks, we calculated from the data of Fig. 2 the 7-day  $\chi^2$  curve<sup>14</sup> (Fig. 3) in the null hypothesis

<sup>14</sup> For the AGILE data, we started with the 1-day binned flux

that the Crab Nebula is constant at its average flux ( $F_s = 220 \times 10^{-8} \text{ ph cm}^{-2} \text{ s}^{-1}$  in the Catalog of Pittori et al. 2009).

We then calculated the probability of obtaining a given  $\chi^2$  (considering the degrees of freedom) in the null hypothesis. If  $\chi_{obs}^2$  is the observed value of  $\chi^2$ ,  $p(\chi^2, n)$  is the probability of obtaining a value of  $\chi^2 \geq \chi_{obs}$ , with  $n$  degrees of freedom. For 7 degrees of freedom, the horizontal dashed lines in Fig. 3 indicate the value of  $\chi^2$  (quantiles) corresponding to the  $3\sigma$ ,  $4\sigma$  and  $5\sigma$  confidence level, respectively. We see that the post-October, 2007 four observations of the Crab Nebula performed by AGILE in the pointing mode are compatible with the average emission within  $1\sigma$ . However, three episodes during the first observation (from MJD  $\simeq 54360$  to MJD  $\simeq 54395$ ) are above  $5\sigma$  with respect to the Crab Nebula average emission.

The lightcurve extending for 20 days including the first pointing, from Sept. 24, 2007 to Oct. 13, 2007, is shown in Figure 4. In the inset we show a zoom of the lightcurve focused on the short variability episodes. Three events stand out above 5 sigma (for a 7-day time bin) in Fig. 3. The most significant corresponds to a flaring sequence, and two other events can be attributed to a less intense but long timescale enhanced emission anticipating the flares, with an average flux of  $\sim 450 \times 10^{-8} \text{ ph cm}^{-2} \text{ s}^{-1}$  and a rise and decay time of the order of several days.

These slow components of enhanced  $\gamma$ -ray emission show features different than those of flares that typically have rise and decay times of the order of 12-24 hr, and peak fluxes ranging from  $F_{p,5} \simeq 800 \times 10^{-8} \text{ ph cm}^{-2} \text{ s}^{-1}$  up to  $F_{p,10} \simeq 2500 \times 10^{-8} \text{ ph cm}^{-2} \text{ s}^{-1}$  (as for the Crab super-flare of Apr. 2011).

These episodes of slow enhanced emission are significant (see discussion below): we call them *waves*. We indicate with  $W_1$  the emission from MJD  $\simeq 54367$  to MJD  $\simeq 54374$ . From MJD  $\simeq 54376$  to MJD  $\simeq 54382$  we observe another event of enhanced emission, that we interpret as a second “wave” with a small flare superimposed at MJD  $\simeq 54381$ . We name this second region  $W_2$ . The 12-hr lightcurve in the inset of Fig. 4 shows that the 2007 peak intensity event, that in our previous analysis (Tavani et al. 2011a) appeared unresolved, is actually composed of three different flaring components, that we indicate by  $F_1$ ,  $F_2$ , and  $F_3$ . Peak fluxes, rise times and decay times (estimated with an exponential fit) for  $F_1$ ,  $F_2$ , and  $F_3$  and for  $W_1$  and  $W_2$  are presented in Tab. 1 and Tab. 3. In order to take into account the number of 1-day maps (trials) carried out in our search for enhanced emission, we also calculated the post-trial significance for  $W_1$  and  $W_2$ , where the post-trial probability is given by  $P_{post} = 1 - (1 - p)^{N_t}$  with  $p$  the pre-trial probability obtained from the  $\chi^2$  test, and  $N_t$  the number of trials. AGILE in pointing mode observed the Crab for a total time of  $\sim 50$  days; considering that the  $\chi^2$  value is calculated over 7 days, the number of trials is  $N_t \simeq 7$ . We find that the post-trial significance is  $P_{post} > 5\sigma$  for both  $W_1$  and  $W_2$ .

The spectral properties of the  $W_1$  and  $W_2$  waves and

data, and then calculated the  $\chi^2$  values summing over 7 days,  $\chi^2 = \sum_{i=1}^7 \frac{(F_o(i) - F_s)^2}{\sigma_i^2}$ , where  $F_o(i)$  is the  $i$ -th observed flux,  $F_s$  is the steady state flux, and  $\sigma_i$  is the  $i$ -th flux error.

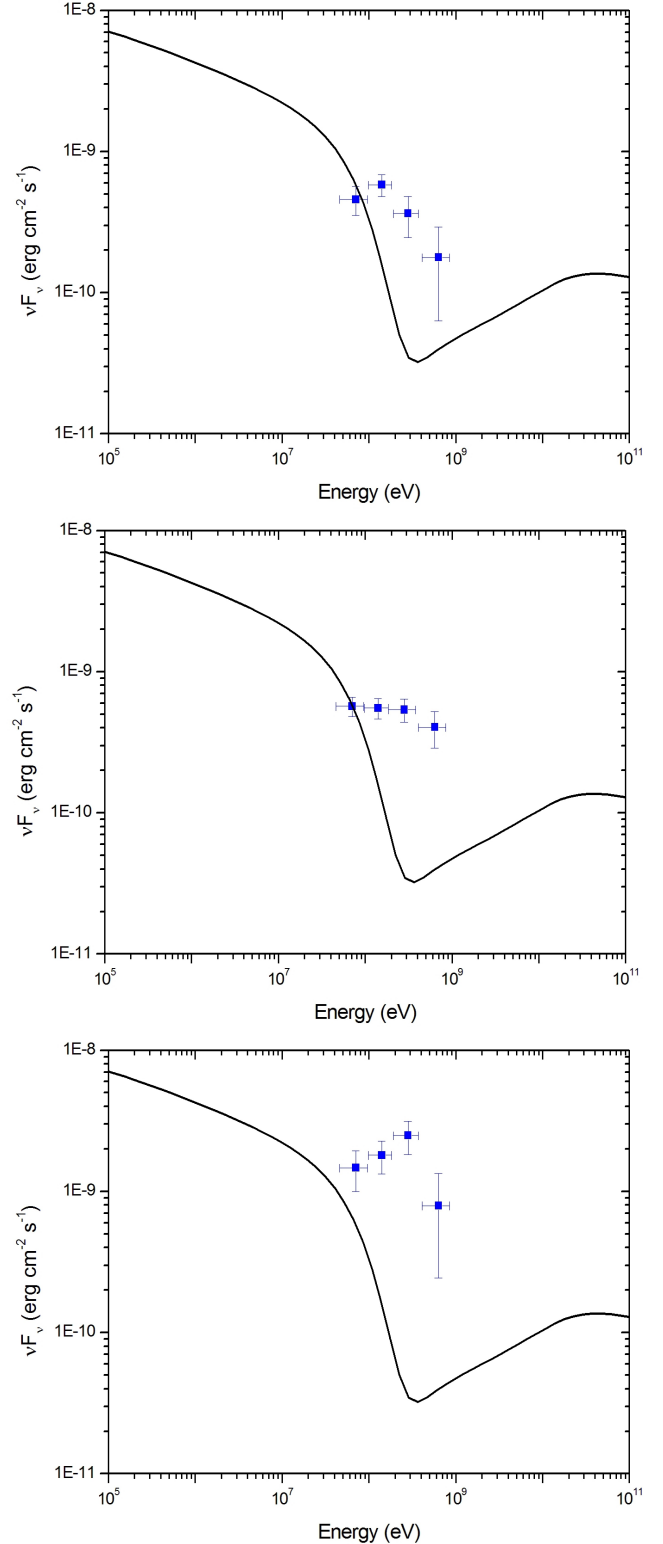


FIG. 5.— AGILE-GRID gamma-ray pulsar-subtracted spectrum of the Crab Nebula  $W_1$  (integrating from MJD = 54368 to MJD = 54374, top panel),  $W_2$  (integrating from MJD = 54376 to MJD = 54382, central panel) and the major flare  $F_2$  (12-hr integration, from MJD = 54382.5 to MJD = 54383.0, bottom panel).

of the flares in September-October 2007 are interesting. Fig. 5 shows the spectral analysis of  $W_1$  (obtained integrating from MJD = 54368 to MJD = 54374),  $W_2$  (ob-

tained integrating from MJD = 54376 to MJD = 54381), and the spectral analysis of  $F_2$  obtained with a 12-hr integration. (We notice that the spectrum of  $W_2$  might be contaminated by presence of the first flare,  $F_1$ ).

We find that the differential particle energy distribution function (per unit volume) can be described by a monoenergetic function,  $dn/d\gamma = K/\alpha \cdot \delta(\gamma - \gamma^*)$ , where  $\gamma$  is the particle Lorentz factor, and  $\gamma^*$  is the monochromatic value of the particle energy. The constant  $K$  is defined in the spherical approximation, with  $\alpha = 1$  in the spherical case, and  $\alpha < 1$  for cylindrical or pancake-like volumes. A power-law distribution and/or a relativistic Maxwellian distribution were also shown to be consistent with the flaring data (Tavani et al., 2011a, Striani et al. 2011b). We adopt here a monochromatic distribution that deconvolved with the synchrotron emissivity leads to an emitted spectrum practically indistinguishable from the relativistic Maxwellian shape (e.g., Striani et al. 2011b, Buehler et al. 2012). This distribution is in agreement with all available gamma-ray data (for both flaring and “wave” behavior, see below), and reflects an important property of the flaring Crab acceleration process (Tavani 2013). In our model we have five free physical parameters: the Lorentz factor  $\gamma^*$ , the local magnetic field  $B$ , the electron density constant  $K$ , the dimension of the emitting region  $l$ , and the Doppler factor  $\delta$ . The values of these parameters are obtained, by means of a multi-parameter fit, from the following quantities (in the observer frame): the position of the peak photon energy,  $E_p \propto \delta \gamma^{*2} B$ , the peak emitted power  $\nu F \propto \delta^4 K / \alpha l^3 B^2 \gamma^{*2}$ , the rise time  $\tau_1 = l / (c\delta)$ , and the cooling time  $\tau_2 = 8.9 \times 10^3 / [(B/\text{Gauss})^2 \gamma^* \delta]$ . We fix the Doppler factor at the value  $\delta = 1$  (relaxing this condition leads to slightly different constraints for  $B$  and  $\gamma^*$  that can be easily calculated without altering the main conclusions of our paper). We determine the characteristic timescales  $\tau_1$  and  $\tau_2$  by a 3-parameter model (see note 1), and from those values we deduce the other physical quantities. We find for  $W_1$  a magnetic field  $B = (0.8 \pm 0.2)$  mG, a Lorentz factor  $\gamma^* = (4 \pm 1) \times 10^9$ , and a typical emitting length range  $l = (0.5 - 1.5) \times 10^{16}$  cm. For  $F_2$ , we find  $B = (1.5 \pm 0.5)$  mG,  $\gamma^* = (3 \pm 1) \times 10^9$ , and  $l = (1.5 \pm 0.7) \times 10^{15}$  cm. In our model, the total number of accelerated particles producing the gamma-ray wave/flaring behavior is in the range  $N \sim (1 - 3) \cdot 10^{38} (\Delta\Omega/4\pi)$ , with  $\Delta\Omega$  the solid angle of the  $\gamma$ -ray emission. It is interesting to note that besides the differing values of the magnetic field and particle densities, the typical Lorentz factor and total number of radiating particles are similar for the “wave”  $W_1$  and the flare  $F_2$ . We find that this is a typical behavior of the transient gamma-ray emission that appears to be well represented by a monochromatic particle distribution function with  $\gamma^* \simeq (3 - 5) \times 10^9$ .

#### 4. SEARCH FOR ENHANCED GAMMA-RAY EMISSION IN THE FERMI-LAT DATA

Motivated by the waves found in the AGILE data, we searched for a similar type of enhanced gamma-ray emission in the publicly available Fermi-LAT data. Fig. 6 shows the lightcurve of the Crab (pulsar + Nebula) during the period Sept. 2008 - May 2012 obtained by a standard unbinned likelihood analysis of the Fermi data (2-day bin). The three major flares from the Crab Neb-

ula detected by Fermi-LAT, and the new low-intensity event recently announced in Jul. 2012 in ATel #4239 (Ojha et al. 2012) are recognizable at MJD  $\sim 54869$ , MJD  $\sim 55459$ , MJD  $\sim 55667$  and MJD  $\sim 56113$ .

Starting with the 2-day bin lightcurve we calculated the  $\chi^2$  distribution based on 8-day integrations, and tested the null hypothesis for a source with a constant average flux  $F_F = (296 \pm 2.5) \times 10^{-8} \text{ ph cm}^{-2} \text{ s}^{-1}$  above 100 MeV for the pulsar plus Nebula signal<sup>15</sup>. We used the same procedure employed for the study of the AGILE data<sup>16</sup>. In Fig. 7 we show the 8-day bin  $\chi^2$  calculated for the whole Fermi-LAT dataset ( $\sim 4$  years). As in Fig. 3, the dashed lines in Figure 7 indicate the  $\chi^2$  corresponding to the  $3\sigma$ ,  $4\sigma$  and  $5\sigma$  confidence level for 4 degrees of freedom. In addition to the three major peaks of the  $\chi^2$  curve (corresponding to the major flares of Feb. 2009, Sept. 2010 and Apr. 2011) we identify several episodes of enhanced gamma-ray emission (above a  $5\sigma$  pre-trial significance) that we call  $W_3, W_4, W_6$  and  $W_7$  in Fig. 8. These episodes have apparent durations in the range from 8 to 50 days (see the complex marked as  $W_3 - W_4$ ), and an average flux in the range  $F = (350 - 500) \times 10^{-8} \text{ ph cm}^{-2} \text{ s}^{-1}$ . The event  $W_7$  is coincident with the very recent enhancement episode detected<sup>17</sup> by Fermi-LAT (Ojha et al., 2012). Fig. 8 shows the detailed lightcurves of the Fermi-LAT wave episodes with the largest post-trial significance<sup>18</sup>.

Fig. 8 shows a remarkable episode of “wave” enhanced emission near MJD = 55000. The Crab was for about 50 days above  $5\sigma$  from its standard gamma-ray flux, with an average flux in this period  $F = (340 \pm 6) \times 10^{-8} \text{ ph cm}^{-2} \text{ s}^{-1}$ . This event appears quite complex<sup>19</sup>. A minor flare (that we mark as  $f^*$ , at MJD  $\sim 54982$ ) anticipates a complex and long emission that we approximate as two “waves”,  $W_3$  and  $W_4$ . The “waves”  $W_3$  and  $W_4$  last for  $\sim 15 - 20$  days each, and show a post-trial significance (on a 8-day timescale) near or above  $5\sigma$  (see also Table 3 in the Appendix). The total episode that includes  $f^*$ ,  $W_3$  and  $W_4$  has a time duration of  $\sim 50$  days, a pre-trial probability  $p = 2 \times 10^{-25}$  and a post-trial significance  $\sigma_{post} > 10$ . For each “wave” that we found at  $5\sigma$  above the Crab average emission, we estimated the rise  $\tau_1$  and the decay time  $\tau_2$ , the average flux, the peak flux, the probability of obtaining the given  $\chi^2$  in the null hypothesis, and the post-trial significance. The rise and decay timescales are estimated with an exponential fit. The results are summarized in Tab. 3.

#### 5. CONSTRAINTS FROM A SYNCHROTRON COOLING MODEL

We can deduce important physical parameters of the

<sup>15</sup> See, e.g., <http://www.asdc.asi.it/fermi2fgl>.

<sup>16</sup> For the Fermi-LAT data, we started with the 2-day binned flux data, and then calculated the  $\chi^2$  values summing over 8 days,  $\chi^2 = \sum_{i=1}^4 \frac{(F_o(i) - F_s)^2}{\sigma_i^2}$ , where  $F_o(i)$  is the  $i$ -th observed flux,  $F_s$  is the steady state flux, and  $\sigma_i$  is the  $i$ -th flux error.

<sup>17</sup> Due to solar panel constraints, this event was unobservable by AGILE.

<sup>18</sup> The post-trial significance was calculated as in the previous Section. Considering four years of Fermi data, and a 8-day time bin, the number of trials turns out to be  $N_t \simeq 180$ .

<sup>19</sup> For simplicity, we use an exponential approximation for the “wave” emission. Admittedly, this approximation for the episode of Fig. 8 centered on MJD = 55000 is not adequate. It is shown in Fig. 8 for illustrative purposes only.



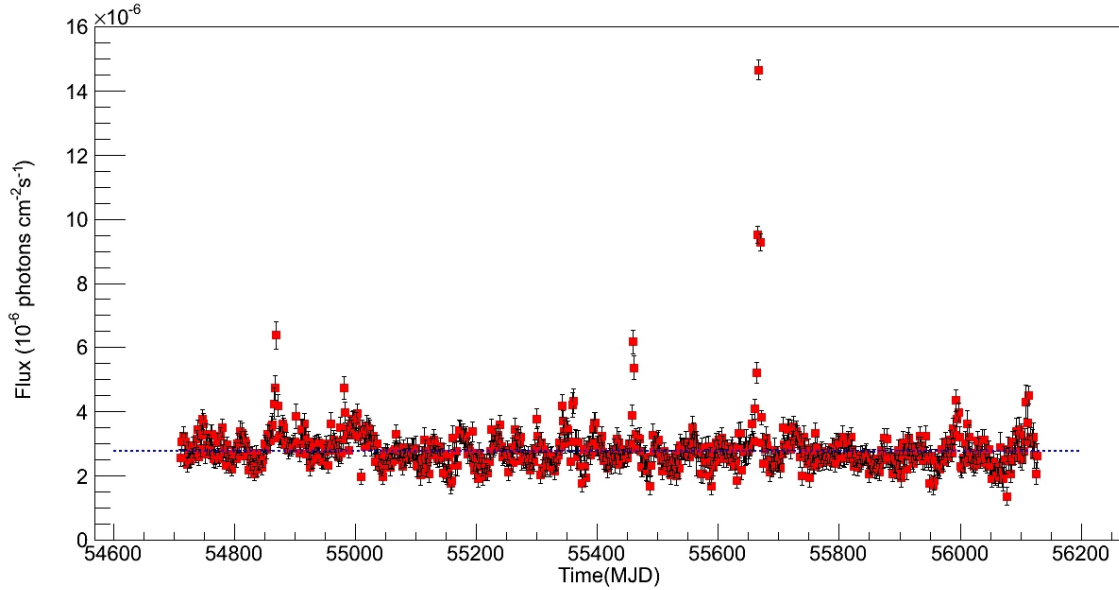


FIG. 6.— Fermi-LAT 2-day bin lightcurve above 100 MeV of the Crab (pulsar plus Nebula) spanning the time period Sept. 2008/Jul. 2012. Results obtained with the publicly available unbinned likelihood analysis software.

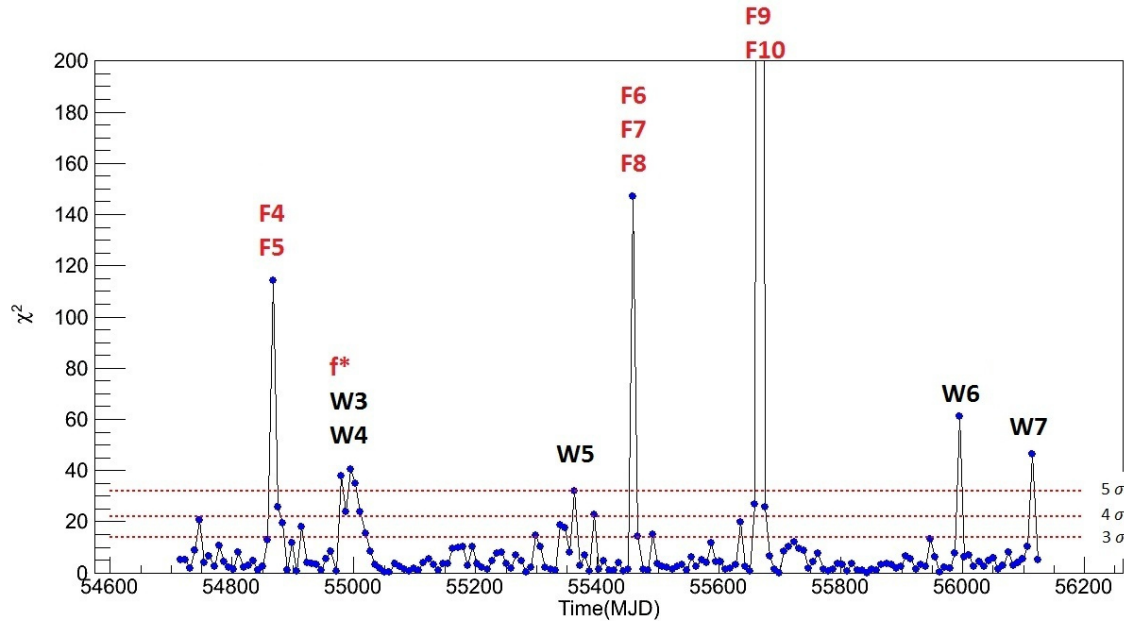


FIG. 7.— Plot of the  $\chi^2$  values (each calculated for 8-day time intervals, based on 2-day binned data) as a function of time for the gamma-ray Fermi-LAT data on the Crab covering the period Sept. 2008/Jul. 2012.

enhanced  $\gamma$ -ray emission by adopting a synchrotron cooling model (see also Tavani et al. 2011a, Vittorini et al. 2011, Striani et al. 2011b). Tables 1, 2, and 3 summarize the relevant information for the major “flares” and “waves”. We constrain the physical quantities of our model as described in sect. 3. We find that for flares lasting 1-2 days the typical length is  $l \simeq (1-2) \times 10^{15}$  cm, the density constant in the range  $K/\alpha = (2-8) \times 10^{-9} \text{ cm}^{-3}$ , the typical Lorentz factor  $\gamma^* = (2.5-4.5) \cdot 10^9$ , and the local magnetic field affecting the cooling phase in the range  $B = (1-2)$  mG. As discussed above, the total number of radiating particles, in case of unbeamed ( $\delta = 1$ ) isotropic

emission, is  $N \sim (1-3) \cdot 10^{38}$ .

For the “wave” episodes, the typical length is  $l > 10^{16}$  cm, the density constant is in the range  $K/\alpha = (2-8) \times 10^{-11} \text{ cm}^{-3}$ , the Lorentz factor  $\gamma^* = (3-5) \cdot 10^9$ , and the local magnetic field in the range  $B = (0.5-1)$  mG. The total number of particles involved is of the same order as in the case of flares.

We show in Fig. 9 a schematic representation of the physical parameter space ( $B$  vs.  $\gamma^*$ ) for the steady emission, waves and flares that are characterized by different and distinct regions. The local magnetic field for “waves” and “flares” is definitely amplified with respect to the

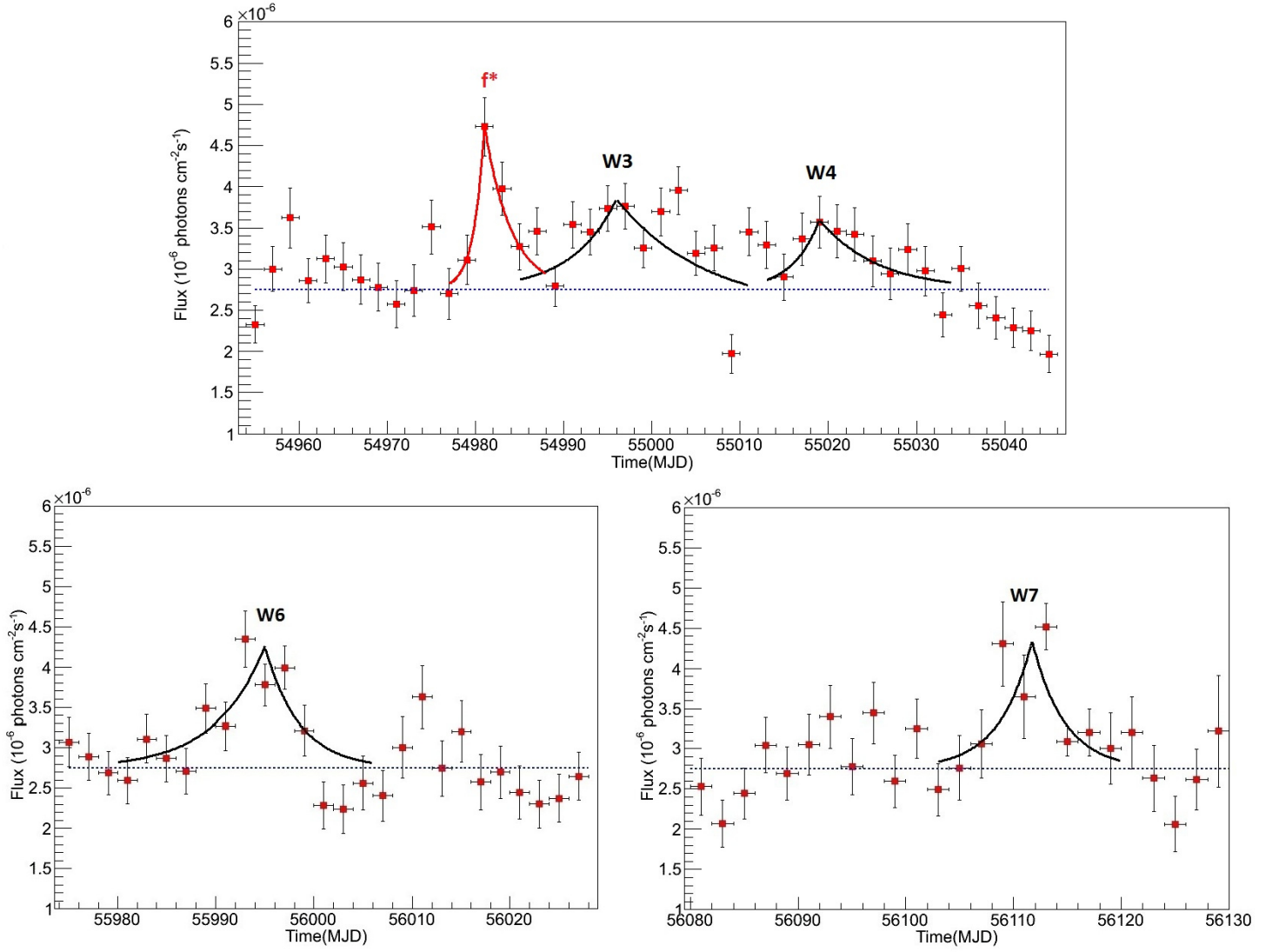


FIG. 8.— The most prominent *wave* episodes in the Fermi-LAT data with more than  $5\sigma$  enhancements above the Crab average emission. 2-day binned gamma-ray flux values (in unit of  $10^{-6} \text{ ph cm}^{-2} \text{ s}^{-1}$ ) above 100 MeV as a function of time. We notice that the event marked as  $f^*$  is intermediate between flares and waves.

TABLE 2  
TABLE OF THE *waves* ABOVE  $5\sigma$  POST-TRIAL FROM THE CRAB AVERAGE EMISSION FOUND IN THE AGILE AND FERMI DATA.

Name	MJD	Duration (days)	$\tau_1$ (days)	$\tau_2$ (days)	Average Flux ( $10^{-8} \text{ ph cm}^{-2} \text{ s}^{-1}$ )	Peak Flux ( $10^{-8} \text{ ph cm}^{-2} \text{ s}^{-1}$ )	Pre-trial p-value	Post-trial significance
$W_1$	54368-54373	5	$2 \pm 1$	$2 \pm 1$	$440 \pm 40$	$670 \pm 200$	$4.5 \times 10^{-8}$	5.0
$W_2$	54376.5-54382.5	6	$2.5 \pm 1$	$2 \pm 1$	$480 \pm 40$	$760 \pm 140$	$3.0 \times 10^{-9}$	5.5
$W_3$	54990-55008	18	$5 \pm 2.5$	$10 \pm 5$	$352 \pm 9$	$380 \pm 30$	$1.0 \times 10^{-8}$	4.6
$W_6$	55988-56000	12	$5 \pm 2.5$	$3.5 \pm 1.5$	$367 \pm 12$	$435 \pm 35$	$1.8 \times 10^{-12}$	6.2
$W_7$	56108-56114	6	$3 \pm 1.5$	$3 \pm 1.5$	$431 \pm 22$	$450 \pm 30$	$1.9 \times 10^{-9}$	5.9

Photon fluxes are obtained for  $E_\gamma > 100 \text{ MeV}$ .



standard average Crab magnetic field ( $\sim 200\mu\text{G}$ ) by a factor 5-10, reflecting the magnetic nature of the instability producing the enhanced  $\gamma$ -ray emission. Remarkably, we find that, within the monochromatic approximation of the enhanced particle energy distribution in agreement with all spectral “wave”/flare data, the Lorentz factor is in the range  $2.5 \cdot 10^9 \leq \gamma^* \leq 5 \times 10^9$  for both “waves” and “flares”. The indication that both “flares” and “waves” have the same characteristic Lorentz factor  $\gamma^*$  suggests a limitation of the acceleration process, most likely induced by radiation reaction. However, the monochromatic vs. a more extended power-law nature of the “wave” emission requires to be tested by additional multifrequency data.

## 6. DISCUSSION AND CONCLUSIONS

In this paper we addressed the issue of the duration and intensity of detectable enhanced gamma-ray emission from the Crab Nebula. By considering AGILE and Fermi-LAT gamma-ray data above 100 MeV we find that the Crab produces a broad variety of enhanced emission. We characterize this enhanced emission as short timescale (1-2 day) “flares” and long timescale (1 week or more) “waves”. Given the current detection level of 1-2 day enhancements (which can be extended to longer timescales of order of 1-2 weeks), we cannot exclude that the Crab is producing an even broader variety (in flux and timescales) of enhanced gamma-ray emission. With the current sensitivities of  $\gamma$ -ray telescopes we can explore an important but necessarily limited range of flux and spectral variations. It is interesting to note that what we called “flares” and “waves” (a somewhat arbitrary division) share the same spectral properties. Given the current gamma-ray sensitivities, we could have detected different spectral behaviors in the energy range 50 MeV - 10 GeV. Most likely, flares and waves are the product of the same class of plasma instabilities that we show acting on different timescales and radiation intensities. The overall detectable transient emission appears to be without any discernible pattern (see, e.g., Fig. 7). Whether or not the instability driver of this process is truly stochastic in flux and timescales will be determined by a longer monitoring of the Crab Nebula. The transient behavior is the topic of current intense theoretical investigation<sup>20</sup> (e.g., Bednarek & Idec 2011, Komissarov & Lyutikov 2011, Uzdensky, Cerutti & Begelman 2011, Cerutti, Uzdensky & Begelman 2012, Bykov et al. 2012, Sturrock & Aschwanden 2012, Clausen-Brown & Lyutikov 2012, Kohri et al. 2012, Lyubarsky 2012, Komissarov 2013, Mignone et al., 2013, Tavani 2013). The

pulsar wind outflow and nebular interaction conditions need to be strongly modified by instabilities in the relativistic flow and/or in the radiative properties. Plasma instabilities possibly related to magnetic field reconnection in specific sites in the Nebula can be envisioned. However, evidence for magnetic field reconnection events in the Crab Nebula is elusive, and no optical or X-ray emission in coincidence with the gamma-ray flaring has been unambiguously detected to date (e.g., Weisskopf et al. 2012).

Both the flaring and “wave” events can be attributed to a population of accelerated electrons consistent with a mono-chromatic or relativistic Maxwellian distribution of typical energy  $\gamma^* \sim (2.5 - 5) \cdot 10^9$ . The magnetic field inducing synchrotron radiation during the decay phase of the waves/flares is substantially larger than in the steady state, as shown in Fig. 9. The range of particle energies reproducing the wave/flare spectra is quite restricted with respect to the steady state, and concentrated towards the maximum value of the overall distribution function. This is an important property of the flaring Crab acceleration mechanism whose maximum energy is most likely limited by radiation reaction.

We also notice that the emitted total energies that can be deduced for the wave ( $\delta E_{\gamma,w}$ ) and flare ( $\delta E_{\gamma,f}$ ) episodes in general satisfy the relation  $\delta E_{\gamma,w} \simeq \delta E_{\gamma,f}$ . The total gamma-ray emitted energy for the wave episode  $W_1$  can be estimated as  $\delta E_{\gamma,w1} \sim 10^{41}$  erg. During the 5 days of the  $W_1$  episode, the total Crab spindown energy is  $E_{sd} \sim 2 \cdot 10^{44}$  erg. Therefore, the observed  $W_1$  efficiency for gamma-ray emission above 100 MeV is  $\varepsilon \sim 5 \cdot 10^{-4}$ . We expect the efficiency of synchrotron emission to be of order of 10% of the particle kinetic energy. Therefore, the energy associated with the wave event  $W_1$ , taken here as an example of Crab “wave” emission, can reach a few percent of the total spindown energy.

We conclude that the Crab “wave” events are highly significant and quite important from the energetic point of view. “Waves” typically imply regions larger than in the case of flares, and smaller average magnetic fields. Their total emitted gamma-ray energy can be comparable with that associated with shorter flares. More observations of this fascinating phenomenon are necessary to improve our knowledge of the flaring Crab.

We thank an anonymous referee for his/her comments. Research partially supported by the ASI grants no. I/042/10/0, and I/028/12/0.

<sup>20</sup> See the reports presented at the meeting “The Flaring Crab: Surprise and Impact”, [www.iasf-roma.inaf.it/Flaring\\_Crab](http://www.iasf-roma.inaf.it/Flaring_Crab).

## REFERENCES

- Abdo, A.A., *et al.*, 2011, *Science*, **331**, 739.  
 Atoyan, A.M. & Aharonian, F.A., 1996, *MNRAS*, **278**, 525.  
 Balbo, M., Walter, R., Ferrigno, C. & Bordas, P., 2011, *A&A*, 527, L4.  
 Bednarek, W., & Idec, W. 2011, *MNRAS*, 414, 2229  
 Bykov, A. M., Pavlov, G. G., Artemyev, A. V., & Uvarov, Y. A. 2012, *MNRAS*, 421, L67  
 Buehler, R., *et al.*, 2010, *Astron. Telegram* 2861.  
 Buehler, R., *et al.*, 2011, *Astron. Telegram* 3276.  
 Buehler, R., Scargle, J. D., Blandford, R. D., *et al.* 2012, *ApJ*, 749, 26  
 Cerutti, B., Uzdensky, D. A., & Begelman, M. C. 2012, *ApJ*, 746, 148  
 Clausen-Brown, E., & Lyutikov, M. 2012, *arXiv:1205.5094*  
 Hays, E., *et al.*, 2011, *Astron. Telegram* 3284.  
 Hester, J.J., P. A. Scowen & R. Sankrit *et al.*, 1995, *ApJ*, **448**, 240.  
 Hester, J.J., Mori, K., Burrows, D. *et al.*, 2002, *ApJ*, **577**, L49.  
 Hester, J.J., 2008, *Annual Rev. Astron. & Astrophys.*, **46**, 127.  
 Kohri, K., Ohira, Y., & Ioka, K. 2012, *MNRAS*, 424, 2249

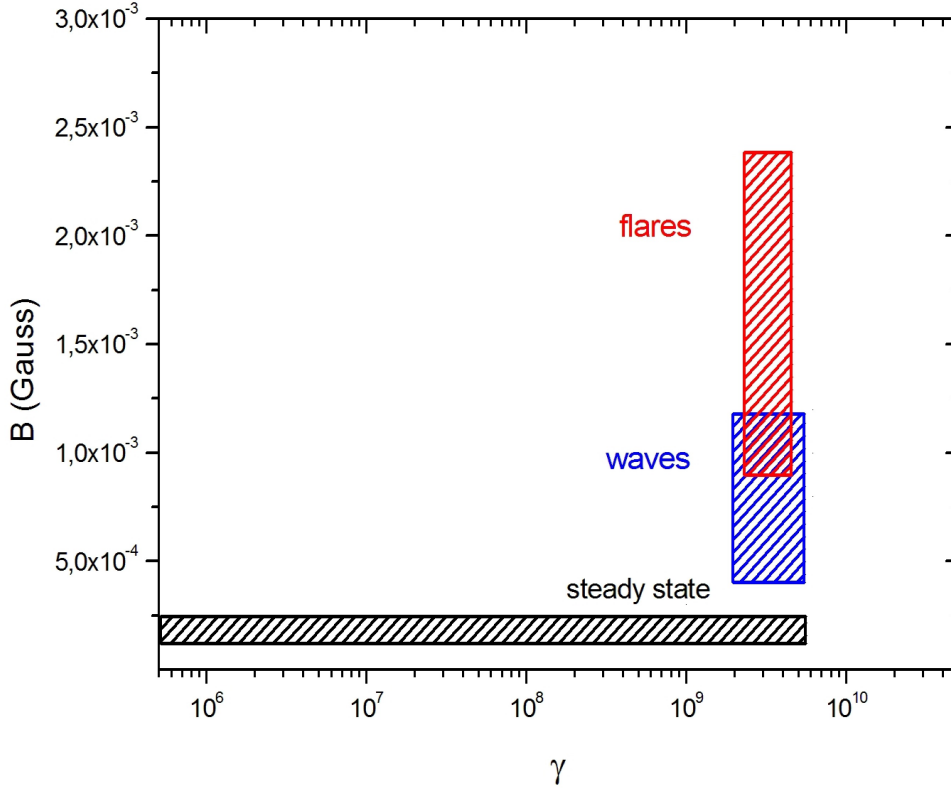


FIG. 9.— Schematic representation of the parameter space ( $B$  vs.  $\gamma$ ) of the Crab Nebula in different  $\gamma$ -ray states for the emission model adopted in this paper (monochromatic particle energy distributions for the “wave” and “flare” states, and power-law distribution for the steady state). For this latter case, the shaded horizontal region indicates the range of Lorentz factors applicable to the power-law distribution. The “wave” spectral shape is poorly constrained, and the effective particle energy distribution of “waves” may extend to the left of the region shaded in blue.

Komissarov, S. S., & Lyutikov, M. 2011, MNRAS, 414, 2017  
 Komissarov, S. S. 2013, MNRAS, 428, 2459  
 Lyubarsky, Y. E. 2012, MNRAS, 427, 1497  
 Meyer, M., Horns, D. & Zechlin, H.S., 2010, A&A, 523, A2.  
 Mignone, A., Striani, E., Ferrari, A., & Tavani, M., in preparation, 2013  
 Norris, J. P., Nemiroff, R. J., Bonnell, J. T., Scargle, J. D., Kouveliotou, C., Paciesas, W. S., Meegan, C. A., & Fishman, G. J. 1996, ApJ, 459, 393  
 Ojha, R., et al., 2012, Astron. Telegram 4239.  
 Pittori, C., Verrecchia, F., Chen, A. W., et al. 2009, A&A, 506, 1563  
 Scargle, J.D., 1969, ApJ, **156**, 401.  
 Striani, E., *et al.*, 2011a, Astron. Telegram 3286.  
 Striani, E., Tavani, M., Piano, G., et al. 2011b, ApJ, 741, L5

Sturrock, P., & Aschwanden, M. J. 2012, ApJ, 751, L32  
 Tavani, M. *et al.*, 2010, Astron. Telegram 2855.  
 Tavani, M., *et al.*, 2011a, Science, **331**, 73.  
 Tavani, M., *et al.*, 2011b, Astron. Telegram 3282.  
 Tavani, M., 2013, in preparation.  
 Tennant, A., *et al.*, 2011, Astron. Telegram 3283.  
 Uzdensky, D. A., Cerutti, B., & Begelman, M. C. 2011, ApJ, 737, L40  
 Vittorini, V., *et al.*, 2011, ApJ, **732**, L22 (V11).  
 Weisskopf, M.C., Hester, J.J., A. F. Tennant, R. F. Elsner, N. S. Schulz *et al.*, 2000, ApJ, **536**, L81.  
 Weisskopf, M. C., Tennant, A. F., Blandford, R., et al. 2012, arXiv:1211.3997.

## APPENDIX

SEARCH FOR  $\gamma$ -RAY “WAVE” EMISSION FROM THE CRAB NEBULA

Table 3 shows results of our complete analysis of “wave” enhanced gamma-ray emission from the Crab Nebula. Seven episodes are identified in the AGILE/Fermi-LAT database with a pre-trial significance larger than  $5\sigma$ . Table 3 provides the corresponding p-values. When selected for post-trial significance (see main text), only a sub-class of events survives as indicated in Table 2. The detectability of the “wave” phenomenon produced by the Crab is clearly limited by the  $\gamma$ -ray sensitivity and exposure characteristics of AGILE and Fermi-LAT. Variable  $\gamma$ -ray emission from the Crab with timing and spectral characteristics different from those addressed in this paper cannot be excluded. Fig. 10 shows the  $\chi^2$  distribution of the Fermi-LAT gamma-ray flux data of the Crab Nebula.

TABLE 3  
TABLE OF THE *waves* ABOVE  $5\sigma$  (PRE-TRIAL) FROM THE CRAB AVERAGE EMISSION FOUND IN THE AGILE AND FERMI DATA.

Name	MJD	Duration (days)	$\tau_1$ (days)	$\tau_2$ (days)	Average Flux ( $10^{-8}$ ph cm $^{-2}$ s $^{-1}$ )	Peak Flux ( $10^{-8}$ ph cm $^{-2}$ s $^{-1}$ )	Pre-trial p-value	Post-trial significance
$W_1$	54368-54373	5	$2 \pm 1$	$2 \pm 1$	$440 \pm 40$	$670 \pm 200$	$4.5 \times 10^{-8}$	5.0
$W_2$	54376.5-54382.5	6	$2 \pm 1$	$2 \pm 1$	$480 \pm 40$	$760 \pm 140$	$3.0 \times 10^{-9}$	5.5
$f^*$	54980.0-54986	6	$1 \pm 0.5$	$2 \pm 1$	$470 \pm 35$	$380 \pm 40$	$8.0 \times 10^{-7}$	4.2
$W_3$	54990-55008	18	$5 \pm 2$	$10 \pm 5$	$352 \pm 9$	$380 \pm 30$	$1.0 \times 10^{-8}$	4.6
$W_4$	55010-55025	15	$3 \pm 1$	$6 \pm 3$	$326 \pm 10$	$360 \pm 30$	$4.6 \times 10^{-7}$	3.8
$W_5$	55358-55362	4	$2 \pm 1$	$2 \pm 1$	$426 \pm 27$	$430 \pm 30$	$5.6 \times 10^{-7}$	3.7
$W_6$	55988-56000	12	$5 \pm 2$	$3 \pm 1$	$367 \pm 12$	$435 \pm 35$	$1.8 \times 10^{-12}$	6.2
$W_7$	56108-56114	6	$3 \pm 1$	$3 \pm 1$	$431 \pm 22$	$450 \pm 30$	$1.9 \times 10^{-9}$	5.9

Photon fluxes are obtained for  $E_\gamma > 100$  MeV. We notice that the event marked as  $f^*$  is intermediate between flares and waves.

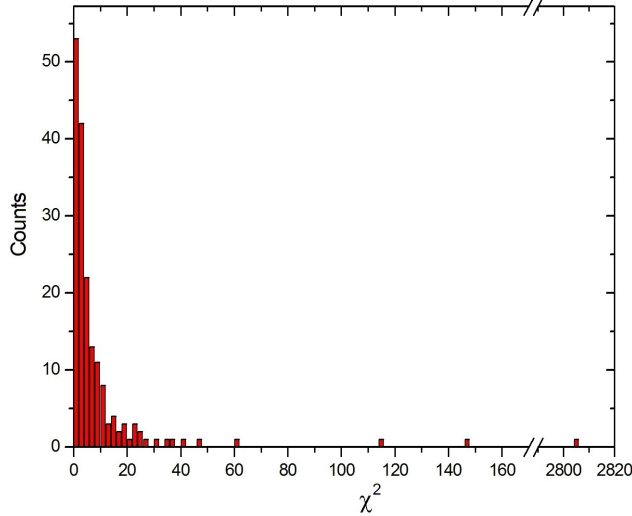


FIG. 10.—  $\chi^2$  distribution of the Fermi-LAT gamma-ray flux data of the Crab Nebula. Each value of  $\chi^2$  is integrated over 8 days.